Chapter 9

Development of All-solid-state Tunable Cr:forsterite Laser System

- *S. P. Sahoo, S. Pradhan, J. Mukherjee & V. S. Rawat*

9.1 Introduction

Tunable lasers like dye lasers are an essential part of any laser-based isotope separation process. The continuous tunability of dye lasers in visible region depend on availability of efficient dye(s) in that particular wavelength region along with the solvents. In this chapter, an all solid state tunable Cr:forsterite laser system is described, which has the potential to replace the copper vapour lasers (CVL) pumped dye laser system for laser isotope separation process. High-power, narrowband, tunable lasers in visible regions have immense application in various fields of spectroscopy, laser-based purification of precious materials, and laser isotope separation. Dye lasers pumped by CVL are the commonly used laser sources for all these applications due to their important properties like, wavelength tunability, high power, and narrow linewidth. However, there are several limitations associated with the liquid dye lasers that necessitate the search for an alternate tunable laser source. These limitations include, the requirement of several organic dyes along with different solvents to cover a wide range of laser spectrum, photodegradation of dyes, health and fire hazards associated with the organic dye solutions, etc. The pump lasers also require big infrastructures for high repetition rate performance. On the other hand, solid-state lasers are compact and simpler, more reliable, have a very less start-up time, and provide ease of operation than liquid and gas lasers. Hence, now-a-days solid-state lasers are becoming more and more popular. The advent of diode-pumped solid-state lasers (DPSSL) has made these all-solid-state lasers widespread. These solid-state lasers are commercially available in both continuous mode (CW) and pulsed mode with a high repetition rate (PRR). Most of these solid-state lasers generate a fixed wavelength and are not tunable. There are only a few solid-state crystals that can be tuned continuously. Most of these tunable solid-state crystals contain aluminium and chromium as the dopant ions which are embedded in different host matrices. Among these, one of the most promising tunable solid-state laser is the Cr:forsterite ($Cr:Mg_2SiO_4$) laser having a wide tuning range that extends from 1130 nm to 1370 nm. The second harmonic of the Cr:forsterite laser (565-685 nm) lies between the fundamental (660-1080 nm) and the

second harmonic (330-540 nm) of Ti:sapphire laser. Hence, by combing these two crystals an all-solid-state laser system can be developed which can generate a wide wavelength spectrum from the near ultraviolet to near-infrared (NIR). The Ti:sapphire laser system along with its second harmonic generation (SHG) is well studied and developed. The narrowband, tunable Ti:sapphire lasers are also commercially available. However, the narrowband, gain-switched Cr:forsterite laser basically in the visible range and in the nanosecond region is not studied in detail. Hence, there was a pressing requirement of developing an all-solid-state tunable, pulsed, narrowband Cr:forsterite laser in the visible range and nanosecond region as an alternative source to the CVL pumped dye lasers. In this chapter, the preliminary development and results of the gain-switched Cr:forsterite laser is presented. This will include the spectroscopic characterization of Cr:forsterite crystal, broadband, and tunable lasing characteristics, spectral and temporal properties, SHG of Cr:forsterite laser, and determination of roundtrip resonator losses and gain coefficient of the Cr:forsterite crystal.

9.2 Spectroscopic Characterization of the Cr:forsterite Crystal

The spectroscopic characterization of the Cr:forsterite crystal was carried out by experimentally measuring the room-temperature absorption and emission spectrum. The Cr:forsterite crystal used in this experiment was grown by Czochralski crystal growth technique. The crystal was in a cuboid form having a dimension of 5 mm x 5 mm x 12 mm and was cut such that both a and b axes are parallel to the end faces. The end faces of the crystal were optically polished and antireflection (AR) coated for the lasing wavelength. The crystal has an absorption coefficient of 1.47 cm^{-1} at 1064 nm for polarization along the b-axis (E ∥ b) and the figure of merit (FOM) of 17. The room temperature absorption and emission spectrum of the crystal were measured using a UV-Vis-NIR spectrometer and shown in Fig. 9.1. For emission spectrum the crystal was excited by the second harmonic of Nd:YAG laser

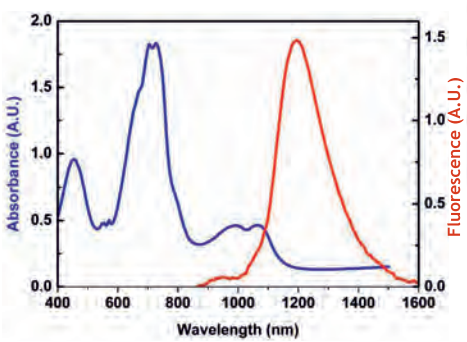

Figure 9.1: Room temperature absorption and emission spectra of Cr:forsterite crystal.

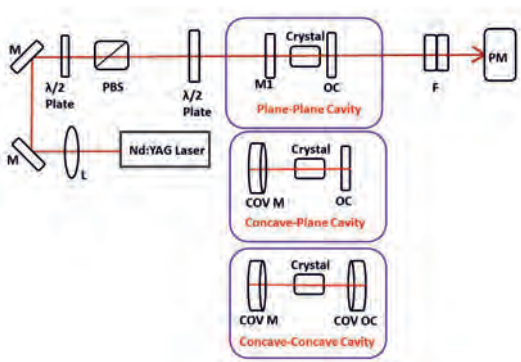

Figure 9.2: Three different interchangeable broadband Cr:forsterite laser resonators: plane-plane, concave-plane and concave-concave.

(532 nm) and the polarization of the crystal was along b-axis of the crystal. The absorption spectrum of the crystal shows it has three absorption peaks, two narrower peaks near at 450 nm and 730 nm and one broad absorption peak between 890–1120 nm. This shows that the Cr:fosterite crystal can be pumped by a large number of laser sources like Nd:YAG laser (both 1064 nm and 532 nm), Yb doped laser, Ti:sapphire laser, diode laser, alexandrite laser,

etc. The emission spectrum of the crystal ranges from 850 nm to 1600 nm which shows that the laser can be tuned over a broader range. It was observed that the absorption of the crystal at the fundamental wavelength of the Nd:YAG laser (1064 nm) is higher than the absorption at its second harmonic (532 nm). Hence, to study the lasing characteristics the Cr:forsterite crystal was pumped with the fundamental wavelength of 1064 nm. It was also observed that when the polarization of the pump beam is along the b-axis of the crystal, the absorption of the crystal is higher than when the pump beam polarization is along the a-axis of the crystal. This was reflected in the observed emission spectrum also in which the fluorescence intensity of the crystal was higher when the pump polarization is along the b-axis of the crystal.

9.3 Lasing Characteristics of Cr:forsterite Laser

The lasing characteristics of the Cr:forsterite crystal were studied by developing both broadband and narrowband tunable laser cavities. In case of the broadband cavity, three different laser resonator geometries, plane-plane, concave-plane and concave-concave were studied to obtain optimal laser performance [114]. The schematic of broadband laser resonator cavities with different geometries are shown in Fig. 9.2. The crystal was pumped by the Nd:YAG laser of 1064 nm having a beam diameter of 8 mm, a pulse repetition rate of 20 Hz, and divergence of 0.5 mrad. The crystal was wrapped inside an aluminium foil mounted inside a copper block. The pump beam was focused using a 1000 mm focal length lens (L) and the crystal was placed away from the focused spot to avoid damage to the crystal. The intensity of the pump beam was varied using a combination of a half-wave plate ($\lambda/2$ plate) and a polarizing beam splitter (PBS). The crystal was oriented for pumping it along the c-axis and the polarization of the pump beam was made collinear to the b-axis of the crystal by using another half-wave plate. The mirror specifications of various resonators used is listed in table

Table 9.1: Mirror specifications of various resonators.

Sr. No	**Resonator geometry**	**HR Mirror Reflectivity @ 1150-1350 nm**	**HR Mirror Transmissivity @ 1064 nm**	**OC Mirror Reflectivity @ 1150-1350 nm**
1.	plane-plane	99%	99%	85%
2.	concave-plane (ROC 100 mm for COV M)	99%	99%	85%
3.	concave-concave (ROC 100 mm for both COV M & OC)	99%	99%	90%

9.1. The power generated from the resonator was monitored through a power meter after passing through a 1064 nm optical filter. The spectral characteristic of the output signal is detected through a spectrophotometer and is shown in Fig. 9.3 which shows the peak wavelength of 1227 nm with bandwidth (FWHM) of ∼25 nm. The input-output characteristics of Cr:forsterite laser for all the three broadband resonators are determined by plotting the output energy of the resonator cavity as a function of absorbed pump energy and is shown in Fig. 9.4. The threshold pump pulse energy and slope efficiency were measured for each resonator cavity. For all the three resonator cavities, plane-plane, concave-plane and concave-concave, the threshold pump pulse energy and slope efficiency measured were 3.5 mJ and 10.6%, 0.4 mJ and 11.3%, and 0.3 mJ and 14.6% respectively. In the case of the concave-plane resonator, the output coupler has a reflectivity of 85% whereas that of for concave-concave resonator the output coupler reflectivity was 90%. Hence, in the case

of the concave-concave resonator, the threshold power is lowest and the slope efficiency is highest [115]. To study the narrowband tunable operation, a Littrow cavity was setup using a blazed diffraction grating of 600 lines/mm. The tunable lasing characteristics in the visible spectrum were studied through the SHG of the Cr:forsterite laser beam. The schematic of the tunable Littrow cavity with its SHG is shown in Fig. 9.5. The fluorescence coming from

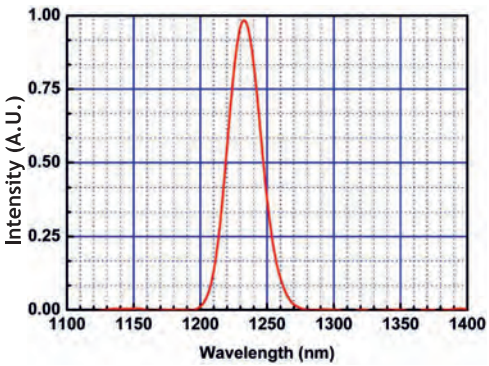

Figure 9.3: Broadband lasing spectrum of Cr: forsterite laser.

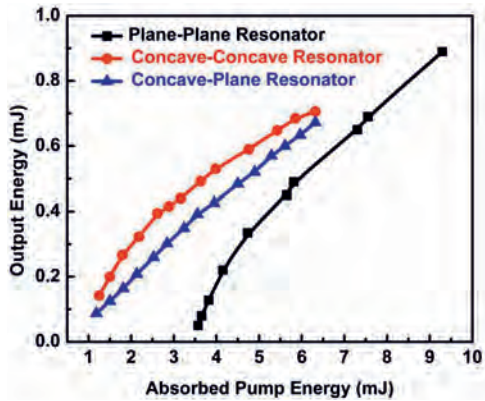

Figure 9.4: Input-output characteristics of different Cr:forsterite broadband laser resonators.

the Cr:forsterite crystal was collimated through a 75 mm focal length lens (L2) and falls on the grating. The fundamental lasing output coming from the cavity was filtered using the pump filter (F1) and sent for its SHG. The SHG unit consists of a short focusing lens (L3) of 30 mm focal length, a BBO crystal, and a dichroic filter (F2). The non-linear BBO (Beta Barium Borate) crystal has a dimension of 4 mm x 4mm x 10 mm and is cut at $\theta = 21°$ and $\phi = 90°$ for type I phase matching. The filter F2 was used to isolate the residual fundamental beam from the SHG beam. The tuning range of the Cr:forsterite fundamental wavelength and its SHG is measured through the spectrometer as shown in Fig. 9.6. The tuning range of the fundamental wavelength of the Cr:forsterite crystal was found to be 1160 nm to 1324 nm having a peak wavelength of 1244 nm. At the peak wavelength, the maximum output energy of 410 μJ was measured for absorbed pump pulse energy 5 mJ which gives the peak efficiency of 8.2%. The SHG is achieved over the entire fundamental wavelength range. For the SHG, the tuning range of 580 nm to 662 nm was measured having a peak wavelength of 622 nm. At the peak wavelength maximum output energy of 36.5 μJ is obtained which gives the second harmonic conversion efficiency of ~9%. The maximum output energy of 549 μJ at the fundamental wavelength and 46.5 μJ at the second harmonic wavelength was obtained for an absorbed pump pulse energy of 8.5 mJ. The FWHM linewidth of the fundamental, as well as the second harmonic laser beam, was measured to be 1.48 nm and 0.83 nm respectively using a laser spectrum analyser (LSA) as shown in Fig. 9.7. These linewidths are limited by grating passband. Further reduction of the laser linewidth is being carried out using higher resolution grating and Fabry-Perot etalons.

9.4 Temporal Properties of Cr:forsterite Laser

The temporal pulse profile of the Cr:forsterite laser was measured using a fast photodiode as shown in Fig. 9.8. The pulse profile of the Cr:forsterite laser shows additional spikes along with the principal pulse. These additional spikes are arising a consequence of laser

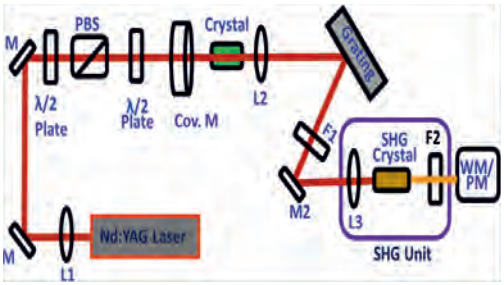

Figure 9.5: Schematic of tunable Cr:forsterite Littrow cavity & its SHG.

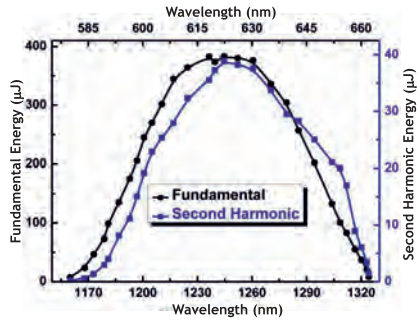

Figure 9.6: Tuning range of fundamental and second harmonic of Cr:forsterite laser.

spiking effect [114]. The pulse width (FWHM) of the principal Cr:forsterite laser pulse was measured to be around 10-15 ns with a jitter of ±2 ns for the 95% reflecting output coupler. The pulse width (FWHM) of the pump laser was around 25 ns with a jitter of ±1 ns. The delay between the pump pulse and the Cr:forsterite principal pulse was measured to be 110 ns which is known as the cavity buildup time. It was also observed that the pulse width of the Cr:forsterite laser was narrower than the pump pulse which is a feature of the gain-switched laser. A four-level rate-equation model was developed to study the spiking behaviour in the Cr:forsterite laser which includes the effect of the excited absorption both at the pump as well as the signal wavelength [114].

9.5 Determination of Gain Coefficient and Roundtrip Resonator Losses

The roundtrip resonator losses (δ) and gain coefficient (g_0) of the Cr:forsterite laser system were measured by using Findlay-Clay analysis in which the threshold input pump energy was measured at different values of the output coupler reflectivity. Conventionally, various output coupler mirrors of different reflectivity are used in this measurement, where output coupler mirrors are required to be changed. Thus, the resonator cavity has to be realigned after each replacement and optimum alignment of the resonator cavity is difficult to be assured each time. It leads to inconsistency in the measurement. A polarization-based laser resonator cavity has been designed and developed in which the reflectivity of the output coupler can be continuously varied without misalignment of the laser cavity. The schematic of the polarization-based laser resonator cavity is shown in Fig. 9.9. The detailed analysis, and characterization of this resonator cavity is explained elsewhere [116]. This resonator cavity provides continuous tuning of various laser and cavity parameters like laser output energy, intracavity energy, laser pulse width, and cavity buildup time preserving the cavity alignment. Using this resonator cavity, the small-signal gain coefficient and roundtrip resonator losses for a Cr:forsterite laser system were measured. This polarization-based laser cavity provides an accurate method of measuring the threshold pump energy for different values of the output coupler reflectivity without disturbing the cavity alignment, unlike the conventional method of changing the output coupler. Hence this method provides precise measurement of threshold pump pulse energy for different output coupler reflectivity. The variation of the output coupler reflectivity ($-\ln R$) as function of the input threshold pump energy (E_{th}) is shown in Fig. 9.10, from which the roundtrip resonator losses (δ) was found to be 0.12 and

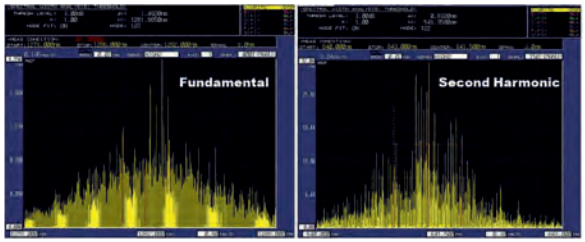

Figure 9.7: Linewidth of fundamental & second harmonic of Cr:forsterite laser.

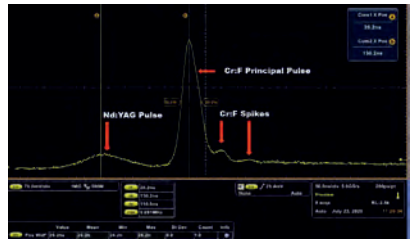

Figure 9.8: Temporal pulse profile of Cr:forsterite laser.

the small-signal gain coefficient (g_0) of the system was found to be 0.076 × E_{in} (cm^{-1}) which is 0.049 cm^{-1} at the cavity threshold pump energy of 0.65 mJ. The absorption coefficient of the crystal at 1064 nm is 1.47 cm^{-1} and FOM is 17. This gives the absorption of the crystal at the laser peak wavelength (1236 nm) is 0.086 cm^{-1} which is 10.3% for 12 mm length of the crystal [115]. The roundtrip resonator losses of the system are 12% which includes 10.3% absorption losses in the crystal itself.

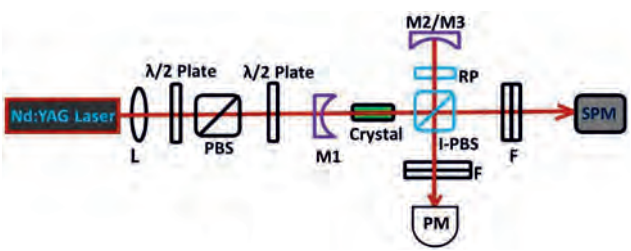

Figure 9.9: Schematic of the polarization-based Cr:forsterite laser resonator cavity.

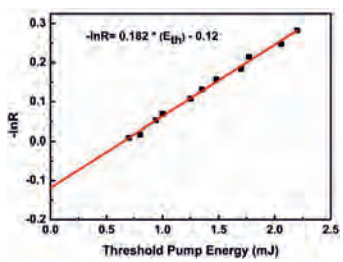

Figure 9.10: Output coupler reflectivity vs. threshold pump energy.

Frequently Asked Questions

Q1. What is an all-solid-state tunable laser system and what is its advantages?

Q2. What should be the properties of a solid-sate gain medium?

Q3. What is the mechanism of a tunable solid-state laser?

Q4. What are available tunable solid-state laser crystals and what is their tuning range?

Q5. What is the figure of merit of a laser crystal?

Q6. What are the roundtrip resonator losses (δ) and gain coefficient (g_0) of a laser system?

Q7. What is the formula for output energy of a resonator cavity in steady-state operation?

Q8. How the roundtrip resonator losses and small signal-gain coefficient of a laser resonator can be obtained?

Q9. What is a gain-switched laser?

Q10. What is the laser spiking behaviour in a solid-state laser and what is its cause?